

# Conditional generation of sub-Poissonian light from two-mode squeezed vacuum via balanced homodyne detection on idler mode

Jaromír Fiurášek

Department of Optics, Palacký University, 17. listopadu 50, 77200 Olomouc, Czech Republic

A simple scheme for conditional generation of nonclassical light with sub-Poissonian photon-number statistics is proposed. The method utilizes entanglement of signal and idler modes in two-mode squeezed vacuum state generated in optical parametric amplifier. A quadrature component of the idler mode is measured in balanced homodyne detector and only those experimental runs where the absolute value of the measured quadrature is higher than certain threshold are accepted. If the threshold is large enough then the conditional output state of signal mode exhibits reduction of photon-number fluctuations below the coherent-state level.

PACS number(s): 42.50.Dv

## I. INTRODUCTION

The possibility of a *conditional generation* of nonclassical states of light has been intensively investigated in recent years. The conditional quantum-state preparation schemes benefit from quantum entanglement between signal mode and an ancilla system (e.g. two output ports of a beam-splitter [1], signal and idler modes in parametric down-conversion [2,3], or cavity mode and an atom in cavity QED [4]). Suppose we measure some observable of the ancilla. The collapse of the ancilla state, caused by the measurement, influences, due to entanglement, the state of the signal mode. In the conditional quantum-state preparation schemes we accept only those experimental runs where the required measurement outcome (or, more generally, a sequence of measurement outcomes) is observed, and we reject all unsuccessful trials.

Based on this general strategy, schemes for conditional generation of Fock states [5], Schrödinger cat states [6,7] and arbitrary superpositions of Fock states in a cavity mode [4,8] have been suggested. In particular, photon-number detection on idler mode of two-mode squeezed vacuum allows one to conditionally generate a highly nonclassical state of signal mode whose Wigner function may be negative near the origin of the phase space [9,10]. Alternatively, one can also use the detected intensity of idler beam as a negative feedback which modulates the intensity of pumping beam [11], or as a trigger of an optical shutter placed in path of pump or signal beams [12]. All these techniques can provide a sub-Poissonian light in signal beam.

A direct detection of the number of photons of the idler mode is not the only possibility here. A quadrature-measurement via balanced homodyne detection would

prepare the signal in squeezed coherent state [2,3]. Similarly, a heterodyne detection on idler leads to coherent state of the signal [2]. Unfortunately, the coherent amplitudes are random, because they are proportional to the value of the detected quadrature of the idler mode. This problem may be circumvented by the feedforward technique where a suitable displacement of the signal is performed thereby compensating the undesired effects of the measurement on the idler mode [2].

In this paper we propose an alternative simple and new way of conditional generation of nonclassical light in the signal mode via homodyne detection of the idler mode. In the suggested scheme, the experimental run is accepted only when the measured quadrature falls within a certain chosen window of quadratures. This guarantees that the conditional state is prepared with finite probability, controlled by the size and position of the quadrature window. For the sake of concreteness, we shall assume that the signal state is successfully generated whenever the absolute value of the detected idler quadrature is higher than certain threshold  $x_0$ . We shall see that the conditional state of signal can exhibit sub-Poissonian photon-number statistics. The amount of suppression of photon-number fluctuations can be controlled by  $x_0$ . There is a trade-off between preparation-probability and the amount of photon-number fluctuations of the generated state. Strong suppression of the fluctuations can be achieved at the expense of a small success rate and vice versa. We address the influence of imperfect detection and show that the nonclassical light can be prepared only if the total efficiency of homodyning is higher than certain threshold.

The paper is organized as follows. In Sec. II we provide a description of the suggested experimental setup. The quantum statistical properties of the conditional state of signal mode are studied in Sec. III. The influence of imperfect homodyne detection is discussed in Sec. IV. Finally, Sec. V contains conclusions.

## II. CONDITIONAL GENERATION

Consider the experimental setup shown in Fig. 1. The two-mode squeezed vacuum state  $|\psi\rangle$  prepared in the nondegenerate parametric amplifier (NOPA) reads [13]

$$\begin{aligned} |\psi\rangle &\equiv \exp\left(r\hat{a}_s^\dagger\hat{a}_i^\dagger - r\hat{a}_s\hat{a}_i\right)|0\rangle_s|0\rangle_i \\ &= \sqrt{1-\lambda}\sum_{n=0}^{\infty}\lambda^{n/2}|n\rangle_s|n\rangle_i, \end{aligned} \quad (1)$$

where  $\hat{a}_s, \hat{a}_i$  ( $\hat{a}_s^\dagger, \hat{a}_i^\dagger$ ) are annihilation (creation) operators of signal and idler modes, respectively,  $|n\rangle_s, |n\rangle_i$  are Fock states of the signal and idler modes,  $r$  is (real) squeezing constant of NOPA and  $\lambda = \tanh^2 r$ . We note that the currently available parametric amplifiers can produce strongly squeezed light. For example, Aytür and Kumar [14] reported a parametric gain  $\cosh^2 r \approx 10$ , which corresponds to  $\lambda \approx 0.9$ .

As illustrated in Fig. 1, the idler mode of two-mode squeezed vacuum is fed to the balanced homodyne detector. The measurement on idler triggers the observation of the signal mode, which is performed only if the detected idler quadrature falls within the chosen window of quadratures  $\mathcal{X}$ . In this way we conditionally generate the output state of the signal mode.

Since it is experimentally challenging to maintain a fixed phase of the local oscillator, we consider the homodyne detection with randomized phases. Positive operator-valued measure (POVM) describing this type of quantum measurements reads

$$\hat{\Pi}_i(x) = \frac{1}{2\pi} \int_0^{2\pi} |x; \phi\rangle_i \langle x; \phi| d\phi, \quad (2)$$

where  $|x; \phi\rangle_i$  is an eigenstate of the quadrature operator  $\hat{x}_{i,\phi} = (\hat{a}_i e^{-i\phi} + \hat{a}_i^\dagger e^{i\phi})/\sqrt{2}$ ,

$$\hat{x}_{i,\phi}|x; \phi\rangle_i = x|x; \phi\rangle_i. \quad (3)$$

The POVM corresponding to the quadrature window  $\mathcal{X}$  can be expressed as

$$\hat{\Pi}_i = \int_{\mathcal{X}} \hat{\Pi}_i(x) dx. \quad (4)$$

The (normalized) reduced density matrix  $\hat{\rho}_s$  of the signal can be obtained by tracing over idler mode

$$\hat{\rho}_s = \frac{\text{Tr}_i \left( \hat{I}_s \otimes \hat{\Pi}_i |\psi\rangle \langle \psi| \right)}{\langle \psi | \hat{I}_s \otimes \hat{\Pi}_i | \psi \rangle}, \quad (5)$$

where  $\hat{I}_s$  is unit operator on Hilbert space of signal mode.

Due to the phase randomized homodyning, density matrix of the conditional state of the signal mode is diagonal in Fock basis,

$$\hat{\rho}_s = \sum_{n=0}^{\infty} p_n |n\rangle_s \langle n|. \quad (6)$$

On inserting the POVM (4) into Eq. (5), we get formula for the photon-number distribution  $p_n$ ,

$$p_n = \frac{1-\lambda}{C(\lambda, \mathcal{X})} \lambda^n q_n, \quad (7)$$

where

$$C(\lambda, \mathcal{X}) \equiv \langle \psi | \hat{I}_s \otimes \hat{\Pi}_i | \psi \rangle = (1-\lambda) \sum_{n=0}^{\infty} \lambda^n q_n \quad (8)$$

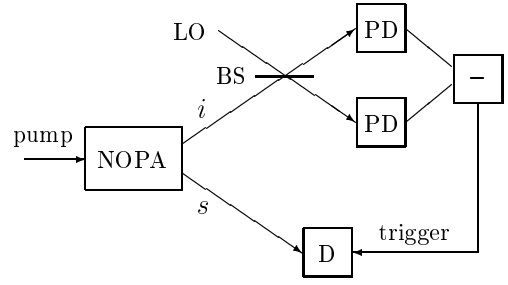


FIG. 1. Scheme of conditional generation of sub-Poissonian light in signal mode from two-mode squeezed vacuum prepared in nondegenerate parametric amplifier (NOPA). A quadrature of idler mode is measured in balanced homodyne detector, which consists of a beam splitter BS, strong coherent local oscillator LO, two photodetectors PD and a subtractor of the two signals. Detected quadrature falling within the chosen window  $\mathcal{X}$  triggers the observation of the signal mode.

is a normalization coefficient and

$$q_n = \int_0^{2\pi} \frac{d\phi}{2\pi} \int_{\mathcal{X}} | \langle x; \phi | n \rangle |^2 dx = \int_{\mathcal{X}} \frac{H_n^2(x) e^{-x^2}}{2^n n! \sqrt{\pi}} dx. \quad (9)$$

Here  $H_n(x)$  denotes Hermite polynomial of variable  $x$ .

### III. PHOTON-NUMBER STATISTICS OF THE CONDITIONAL STATE

So far we have assumed an arbitrary  $\mathcal{X}$ . In what follows, we analyze the case where the conditional state of signal mode is successfully generated if the absolute value of the idler quadrature is higher than certain lower bound  $x_0$ . In this case we can write,

$$q_n = \frac{2}{2^n n! \sqrt{\pi}} \int_{x_0}^{\infty} H_n^2(x) e^{-x^2} dx. \quad (10)$$

The normalization factor  $C(\lambda, x_0)$  represents the probability of conditional generation of the output state (5), i.e. the probability that the absolute value of the measured quadrature of the idler would be larger than  $x_0$ . The idler mode is in thermal (chaotic) state and its quadrature component  $\hat{x}_{i,\phi}$  exhibits Gaussian distribution with zero mean and variance  $(1+\lambda)/[2(1-\lambda)]$ . The probability that  $|x| > x_0$  can be thus expressed as

$$C(\lambda, x_0) = \frac{2}{\sqrt{\pi}} \sqrt{\frac{1-\lambda}{1+\lambda}} \int_{x_0}^{\infty} \exp\left(-x^2 \frac{1-\lambda}{1+\lambda}\right) dx. \quad (11)$$

After a straightforward integration we arrive at

$$C(\lambda, x_0) = 1 - \text{erf}\left(x_0 \sqrt{\frac{1-\lambda}{1+\lambda}}\right), \quad (12)$$

where the error function is defined as

$$\text{erf}(x) = \frac{2}{\sqrt{\pi}} \int_0^x e^{-y^2} dy. \quad (13)$$

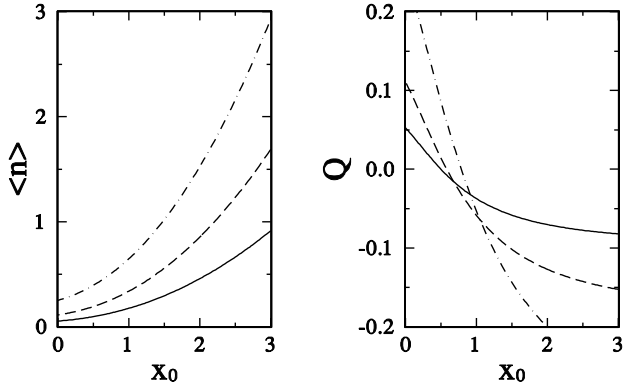


FIG. 2. Mean photon number  $\langle \hat{n} \rangle$  and Mandel  $Q$ -factor versus  $x_0$  for three different squeezing parameters  $\lambda = 0.05$  (solid line),  $\lambda = 0.1$  (dashed line) and  $\lambda = 0.2$  (dot-dashed line).

The function  $C(\lambda, x_0)$  contains a complete information about the quantum-statistical properties of the state (5). From the definition (8) we can deduce that  $C(\lambda, x_0)$  is a generating function of moments of the photon number distribution (7),

$$\langle \hat{n}^k \rangle = \frac{1 - \lambda}{C(\lambda, x_0)} \left( \lambda \frac{d}{d\lambda} \right)^k \left[ \frac{C(\lambda, x_0)}{1 - \lambda} \right]. \quad (14)$$

Also the normally ordered moments can be determined from  $C(\lambda, x_0)$ ,

$$\langle : \hat{n}^k : \rangle \equiv \left\langle \frac{\hat{n}!}{(\hat{n} - k)!} \right\rangle = \frac{(1 - \lambda)\lambda^k}{C(\lambda, x_0)} \frac{d^k}{d\lambda^k} \left[ \frac{C(\lambda, x_0)}{1 - \lambda} \right]. \quad (15)$$

In particular, we obtain expressions for the mean photon number

$$\langle \hat{n} \rangle = \frac{\lambda}{1 - \lambda} + \frac{2\lambda x_0 C^{-1}(\lambda, x_0)}{\sqrt{\pi}[(1 - \lambda)(1 + \lambda)^3]^{1/2}} \exp\left(-x_0^2 \frac{1 - \lambda}{1 + \lambda}\right) \quad (16)$$

and second factorial moment

$$\langle : \hat{n}^2 : \rangle = \frac{2\lambda^2}{(1 - \lambda)^2} + \sqrt{\frac{1 - \lambda}{1 + \lambda}} \frac{2x_0\lambda^2}{\sqrt{\pi}(1 - \lambda^2)C(\lambda, x_0)} \times \left[ \frac{1 + 4\lambda}{1 - \lambda^2} + \frac{2x_0^2}{(1 + \lambda)^2} \right] \exp\left(-x_0^2 \frac{1 - \lambda}{1 + \lambda}\right). \quad (17)$$

The conditional output states  $\hat{\rho}_s$  can be highly nonclassical, exhibiting sub-Poissonian statistics. The suppression of photon-number fluctuations can be conveniently characterized by Mandel  $Q$ -factor [15]

$$Q = \frac{\langle : (\Delta \hat{n})^2 : \rangle}{\langle \hat{n} \rangle} = \frac{\langle \hat{n}^2 \rangle - \langle \hat{n} \rangle^2}{\langle \hat{n} \rangle} - 1. \quad (18)$$

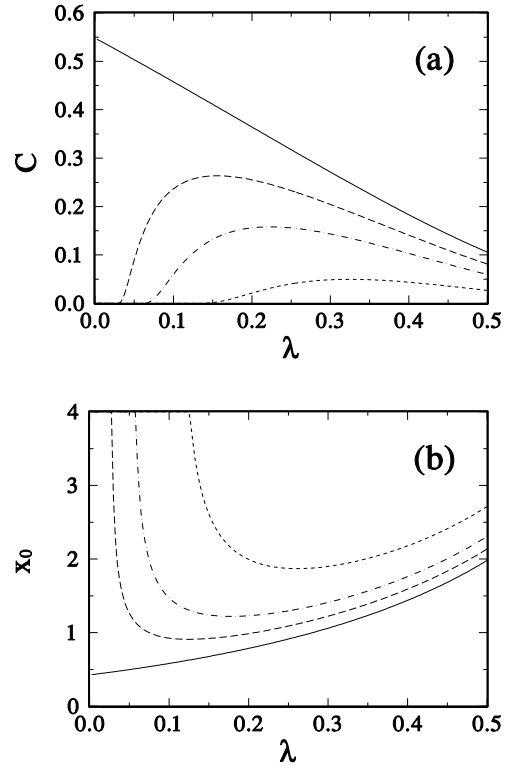


FIG. 3. (a) The probability of conditional generation of state with  $Q = 0$  (solid line),  $Q = -0.05$  (dashed line),  $Q = -0.1$  (dot-dashed line), and  $Q = -0.2$  (short-dashed line). Figure (b) shows the corresponding values of  $x_0$ .

It holds that  $Q \geq -1$  and the equality is achieved for Fock state. The light is sub-Poissonian when the photon-number variance  $\langle (\Delta \hat{n})^2 \rangle$  is less than the mean number of photons  $\langle \hat{n} \rangle$ . This is indicated by negative value of  $Q$ . The statistics are Poissonian when  $Q = 0$  and super-Poissonian if  $Q > 0$ .

The dependence of the mean photon number (16) and the  $Q$ -factor (18) on the lower bound  $x_0$  is plotted in Fig. 2 for three different values of  $\lambda$ . We can see that  $\langle \hat{n} \rangle$  monotonically grows with  $x_0$  while  $Q$  monotonically decreases and eventually becomes negative. The figure clearly indicates that the states  $\hat{\rho}_s$  can possess sub-Poissonian statistics. However, we should be concerned with the probability  $C(\lambda, x_0)$  of generation of such nonclassical states.

Figure 3a shows dependence of this probability on  $\lambda$  for four different  $Q$ -factors. The corresponding values of  $x_0$  required for reaching given  $Q$  are displayed in Fig. 3b. Consider first the boundary case when the photon-number fluctuations are suppressed to the level of Poissonian distribution, hence  $Q = 0$ . The probability of generation can be almost 55% for weakly squeezed states ( $\lambda \ll 1$ ) and decreases with growing  $\lambda$ . In agreement with Fig. 2b, the  $x_0$  required for achieving  $Q = 0$  increases with  $\lambda$ . It is interesting that there is a lower bound on  $x_0$  as  $\lambda \rightarrow 0$ . In order to suppress the fluctuations to

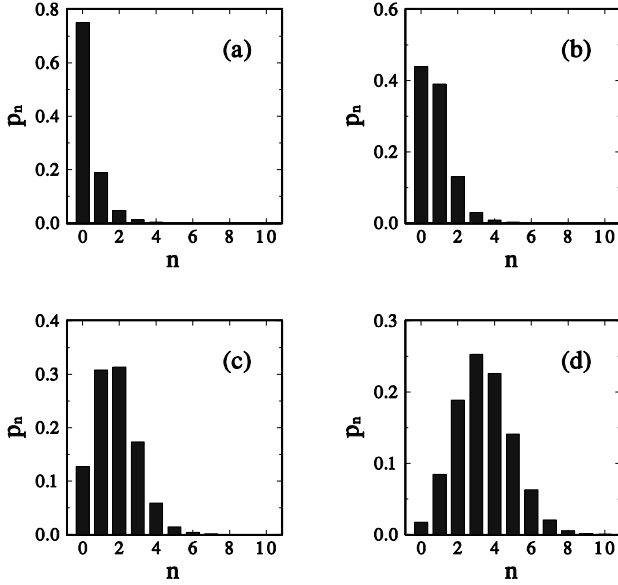


FIG. 4. Photon-number distribution of the conditional state  $\hat{\rho}_s$  for  $\lambda = 0.25$  and (a)  $x_0 = 0$ , (b)  $x_0 = 1$ , (c)  $x_0 = 2$ , and (d)  $x_0 = 3$ .

Poissonian level, we need finite  $x_0$  even for very weak squeezing. This minimum  $x_{0,\min}$  can be determined if we consider the formulas (16), (17) and (18) in the limit  $\lambda \rightarrow 0$ . It follows that  $x_{0,\min}$  is a root of a transcendent equation

$$\left(1 + \frac{2x_0 e^{-x_0^2}}{\sqrt{\pi}[1 - \operatorname{erf}(x_0)]}\right)^2 = 2 + \frac{2x_0(1 + 2x_0^2)}{\sqrt{\pi}[1 - \operatorname{erf}(x_0)]} e^{-x_0^2},$$

whose numerical solution provides  $x_{0,\min} = 0.4248$ .

Assume now that we want to generate a nonclassical state with negative  $Q$ . Figure 3 reveals that for each  $Q < 0$  there is certain optimal value of  $\lambda$  which allows us to generate this state with highest probability. The peak in probability roughly corresponds to the minimum of  $x_0$  but those two extrema do not coincide.

Having investigated the photon-number variance we turn our attention to the photon-number distribution itself. The coefficients  $q_n$  can be calculated from  $C(\lambda, x_0)$  as follows,

$$q_n = \frac{1}{n!} \frac{d^n}{d\lambda^n} \left[ \frac{C(\lambda, x_0)}{1 - \lambda} \right] \Big|_{\lambda=0}. \quad (19)$$

This formula, however, is not very convenient for practical calculations. Therefore we present a different derivation of  $q_n$  which leads to formulas suitable for numerical processing. In order to perform the integration in Eq. (10), we invoke the generating function for Hermite polynomials,

$$e^{-h^2 + 2hx} = \sum_{n=0}^{\infty} \frac{1}{n!} H_n(x) h^n \quad (20)$$

and rewrite Eq. (10) as

$$q_n = \frac{1}{2^n n!} \frac{\partial^{2n}}{\partial h^n \partial k^n} \int_{x_0}^{\infty} e^{-h^2 + 2hx} e^{-k^2 + 2kx} e^{-x^2} dx \Big|_{h=k=0}. \quad (21)$$

After some algebra we find that

$$q_n = \frac{1}{2^n n!} \frac{\partial^{2n}}{\partial h^n \partial k^n} [e^{2hk} [1 - \operatorname{erf}(x_0 - h - k)]] \Big|_{h=k=0}. \quad (22)$$

On performing the differentiation we finally arrive at

$$q_n = 1 - \operatorname{erf}(x_0) + \frac{e^{-x_0^2}}{\sqrt{\pi}} \sum_{j=0}^{n-1} \frac{2^{-j}}{(j+1)!} H_j(x_0) H_{j+1}(x_0). \quad (23)$$

This expression looks particularly simply when rewritten as a recurrence relation,

$$q_n = q_{n-1} + \frac{e^{-x_0^2}}{\sqrt{\pi} 2^{n-1} n!} H_{n-1}(x_0) H_n(x_0), \quad (24)$$

starting with  $q_0 = 1 - \operatorname{erf}(x_0)$ .

Figure 4 illustrates how the shape of the photon number distribution of  $\hat{\rho}_s$  changes with  $x_0$ . When  $x_0 = 0$  and all quadratures are accepted, the signal mode is in thermal state with mean number of chaotic photons  $\langle \hat{n} \rangle = \lambda/(1 - \lambda)$  and positive  $Q$ -factor ( $Q_a = 0.333$ ), see Fig. 4a. This initially super-Poissonian distribution becomes narrower when the lower bound of accepted quadratures  $x_0$  is increased and the statistics shown in Figs 4b-d are sub-Poissonian, as indicated by negative  $Q$ -factors ( $Q_b = -0.026$ ,  $Q_c = -0.216$ , and  $Q_d = -0.297$ ). The selection conditioned by quadrature measurements suppresses the contribution of vacuum and low Fock states and  $p_n$  becomes peaked about  $n$  which grows with  $x_0$ .

These changes in the form of the photon-number distribution are reflected in the shape of quasidistributions, which are phase space representations of the quantum state. The quasidistributions for  $\hat{\rho}_s$  are axially symmetric around the origin of phase space because the density matrix  $\hat{\rho}_s$  is diagonal in Fock basis and does not carry any information about phase. The Husimi quasidistribution  $W_{\mathcal{A}}(\alpha) = \pi^{-1} \langle \alpha | \hat{\rho}_s | \alpha \rangle$  corresponding to states from Figs. 4a and 4c is plotted in Fig. 5. The quasidistribution of thermal (chaotic) state shown in Fig. 5a has Gaussian shape and is peaked at the origin of the phase space. On the other hand,  $W_{\mathcal{A}}$  depicted in Fig. 5b has a clear dip in the origin and is peaked at a nonzero radius.

Although the conditional state  $\hat{\rho}_s$  can be nonclassical, its Wigner function  $W_s(x_s, p_s)$  is always positive. This should be contrasted with conditional generation based on photodetection on the idler, which may lead to states

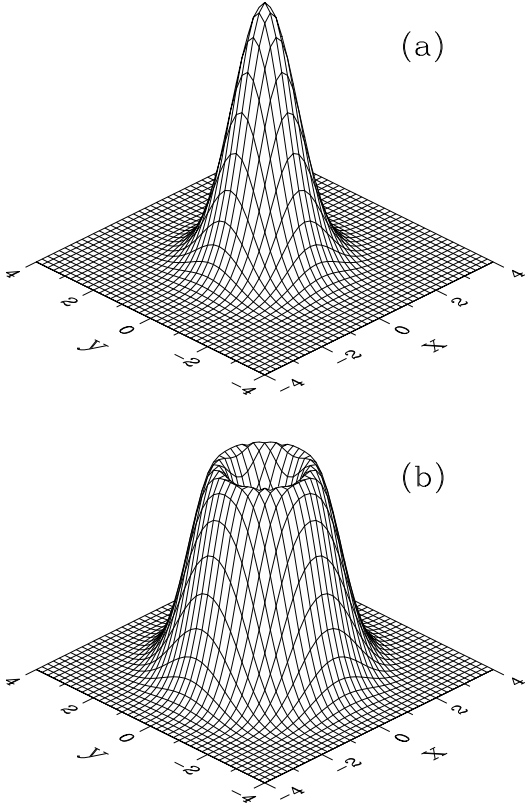


FIG. 5. The Husimi quasidistributions of the state  $\hat{\rho}_s$  for  $\lambda = 0.25$  and (a)  $x_0 = 0$ , (b)  $x_0 = 2$ .

with negative Wigner function [9,10]. The positivity of  $W_s$  can be proved by recalling that the trace of two operators can be evaluated by integrating the product of their Wigner functions over the whole phase space. The Wigner representations of the two-mode squeezed vacuum (1) and POVM (4) are both positive. Taking into account the definition (5) of  $\hat{\rho}_s$ , we immediately conclude that the Wigner function  $W_s$  of the state  $\hat{\rho}_s$  must be positive. In this context we can say that direct photodetection by avalanche photodiode is, in certain sense, more non-classical than balanced homodyne because the Wigner function of the operator  $\hat{\Pi} = \hat{I} - |0\rangle\langle 0|$  is negative in some regions of phase space.

#### IV. IMPERFECT HOMODYNE DETECTION

So far, we have assumed an ideal homodyne detector with unit efficiency. Let us now analyze the influence of imperfect detection with efficiency  $\eta < 1$  on the properties of conditional state of signal mode. We can expect that the nonclassical properties of  $\hat{\rho}_s$  will diminish with decreasing  $\eta$  but we shall see that the suppression of non-classicality is not severe.

A realistic homodyne detector can be modelled by an ideal homodyne detector whose signal input is preceded by a beam splitter, where the signal mode is mixed with

an auxiliary mode which is in chaotic state. The detected quadrature can be thus expressed as [16]

$$\hat{x}_{i,\eta,\phi} = \sqrt{\eta}\hat{x}_{i,\phi} + \sqrt{1-\eta}\hat{x}_{\text{aux}}. \quad (25)$$

In our case the quadrature  $\hat{x}_{i,\eta,\phi}$  has again a Gaussian distribution with zero mean and variance which does not depend on  $\phi$ ,

$$\langle(\Delta\hat{x}_{i,\eta})^2\rangle = \frac{1 + 2\bar{n}(1-\eta) + \lambda[2\eta(1+\bar{n}) - 1 - 2\bar{n}]}{2(1-\lambda)}, \quad (26)$$

where  $\bar{n}$  is mean number of chaotic photons in the auxiliary mode. Making use of the formula (26) we can derive the probability that the absolute value of the measured idler quadrature is higher than the threshold  $x_0$ ,

$$C(\lambda, x_0, \eta, \bar{n}) = 1 - \text{erf}\left(\frac{x_0}{\sqrt{2\langle(\Delta\hat{x}_{i,\eta})^2\rangle}}\right). \quad (27)$$

In what follows we shall assume that the auxiliary mode is in vacuum state, hence  $\bar{n} = 0$  and Eq. (27) simplifies to

$$C(\lambda, x_0, \eta) = 1 - \text{erf}\left(x_0\sqrt{\frac{1-\lambda}{1+(2\eta-1)\lambda}}\right). \quad (28)$$

In the limit of ideal detector,  $\eta = 1$ , this expression reduces to Eq. (12). We may utilize the formulas (14), (15) and calculate the moments of the photon number distribution (7). After some algebra we obtain

$$\langle\hat{n}\rangle = \frac{\lambda}{1-\lambda} + \frac{2\eta\lambda x_0 C^{-1}(\lambda, x_0, \eta)}{\sqrt{\pi}[(1-\lambda)(1+(2\eta-1)\lambda)^3]^{1/2}} \times \exp\left(-x_0^2\frac{1-\lambda}{1+(2\eta-1)\lambda}\right), \quad (29)$$

$$\begin{aligned} \langle:\hat{n}^2:\rangle &= \frac{2\lambda^2}{(1-\lambda)^2} + \frac{2\eta x_0 \lambda^2 C^{-1}(\lambda, x_0, \eta)}{\sqrt{\pi}[(1-\lambda)[1+(2\eta-1)\lambda]^3]^{1/2}} \\ &\times \left[ \frac{4-3\eta+4(2\eta-1)\lambda}{(1-\lambda)(1+(2\eta-1)\lambda)} + \frac{2\eta x_0^2}{[1+(2\eta-1)\lambda]^2} \right] \\ &\times \exp\left(-x_0^2\frac{1-\lambda}{1+(2\eta-1)\lambda}\right). \end{aligned} \quad (30)$$

The POVM describing homodyne detection with realistic detector can be expressed as

$$\hat{\Pi}_{i,\eta} = \int_{\mathcal{X}} \hat{\Pi}_i(x_\eta) dx_\eta, \quad (31)$$

where  $\hat{\Pi}_i(x_\eta)$  reads

$$\hat{\Pi}_i(x_\eta) = \frac{1}{2\pi} \frac{1}{\sqrt{\pi(1-\eta)}} \times \int_0^{2\pi} \int_{-\infty}^{\infty} |x'; \phi\rangle_i \langle x'; \phi| e^{-(x-\sqrt{\eta}x')^2/(1-\eta)} d\phi dx'. \quad (32)$$

The coefficients  $q_n$  in the photon-number distribution (7) may be again calculated in a similar way as in the case of ideal detector. After a long but straightforward algebra we arrive at recurrence relation for  $q_n$ ,

$$q_n = q_{n-1} + \frac{\eta}{\sqrt{\pi}} e^{-x_0^2} \sum_{k=0}^{n-1} \left(\frac{\eta}{2}\right)^{n-k-1} \frac{(1-\eta)^k}{(n-k)!} \times \binom{n-1}{k} H_{n-1-k}(x_0) H_{n-k}(x_0). \quad (33)$$

where we start from  $q_0 = 1 - \text{erf}(x_0)$ .

The detrimental effect of  $\eta < 1$  on the suppression of photon-number fluctuations can be deduced from Fig. 6. In Fig. 6a we plot the probability  $C(\lambda, x_0, \eta)$  of generation of the state with Poissonian fluctuations ( $Q = 0$ ). We can see that the probability reduces with decreasing  $\eta$ . Our numerical calculations reveal that we cannot achieve  $Q = 0$  for any  $\lambda$  when  $\eta < 0.5$ . Figure 6b shows the probability of preparation of a state with sub-Poissonian statistics ( $Q = -0.05$ ). As  $\eta$  diminishes, the maximum probability of generation decreases and the optimal  $\lambda$  increases.

We can provide a simple argument explaining why non-classical light cannot be generated when  $\eta < 1/2$ . To this point let us assume that the homodyne detector in Fig. 1 is replaced with heterodyne detector measuring projections to coherent states,  $\hat{\Pi}_i(\alpha) = \pi^{-1} |\alpha\rangle_i \langle \alpha|$ . Suppose that the output signal is accepted only when the absolute value of the real part of measured  $\alpha$  is larger than  $\alpha_0 \geq 0$ . Since the idler is in chaotic state, its  $Q$ -function is Gaussian and we may express the probability that  $|\text{Re}(\alpha)| > \alpha_0$  as

$$\tilde{C}(\lambda, \alpha_0) = \frac{2(1-\lambda)}{\pi} \int_{-\infty}^{\infty} \int_{\alpha_0}^{\infty} e^{-(1-\lambda)(\alpha_R^2 + \alpha_I^2)} d\alpha_R d\alpha_I, \quad (34)$$

$$\tilde{C}(\lambda, \alpha_0) = 1 - \text{erf}(\alpha_0 \sqrt{1-\lambda}).$$

We can see that  $\tilde{C}(\lambda, \alpha_0) \equiv C(\lambda, x_0 = \alpha_0, \eta = 0.5)$  hence the photon-number statistics of conditional signal state generated via heterodyne detection on idler coincides with statistics of conditional signal state prepared by means of homodyne detection on idler with efficiency 0.5. After the detection of  $\hat{\Pi}_i(\alpha)$  the signal mode is projected to coherent state with complex amplitude  $\alpha_s = \sqrt{\lambda}\alpha^*$  [2]. Thus the conditional state prepared by heterodyne detection on idler is a stochastic mixture of coherent states and cannot exhibit any nonclassical features. Assume now that the auxiliary mode in Eq. (25)

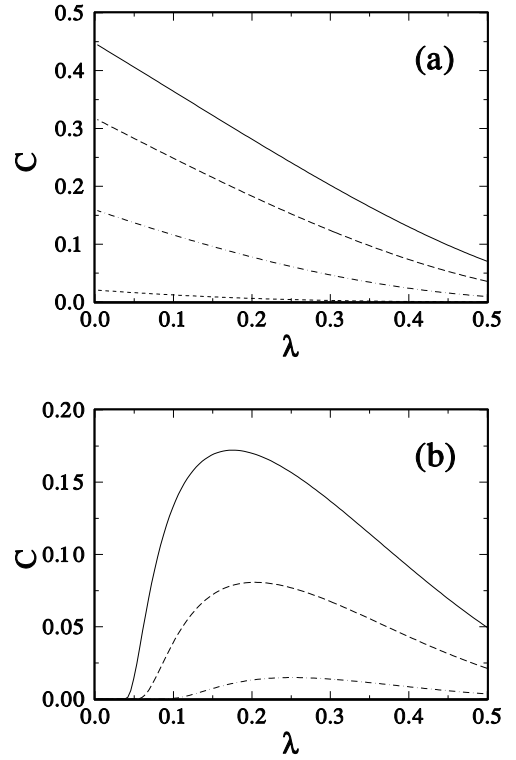


FIG. 6. The probability of generation of state with Mandel  $Q$ -factor (a)  $Q = 0$  and (b)  $Q = -0.05$  is plotted for four different detection efficiencies  $\eta = 0.9$  (solid line),  $\eta = 0.8$  (dashed line),  $\eta = 0.7$  (dot-dashed line) and  $\eta = 0.6$  (short-dashed line).

is in thermal state. When we look at the formula (27), we find that  $C(\lambda, x_0, \eta, \bar{n})$  has the same form as  $\tilde{C}(\lambda, \alpha_0)$  in Eq. (34) when

$$\eta = \eta_{\text{th}} \equiv \frac{1 + 2\bar{n}}{2 + 2\bar{n}}. \quad (35)$$

If  $\eta < \eta_{\text{th}}$ , then the balanced homodyning is formally equivalent to heterodyning with detection efficiency lower than unity. Thus we conclude that the sub-Poissonian light can be conditionally generated only when  $\eta > \eta_{\text{th}}$  holds. The threshold efficiency  $\eta_{\text{th}}$  is lowest when the auxiliary mode is in vacuum state and  $\eta_{\text{th}} = 0.5$ . The threshold  $\eta_{\text{th}}$  increases with  $\bar{n}$  and approaches 1 for large  $\bar{n}$ .

In the experiments, the efficiency is reduced mainly due to only partial overlap between the measured mode and local-oscillator mode. If the overlap is good, then  $\eta$  can be very high. For example, in the single-mode optical homodyne tomography [17], the efficiency  $82\% \pm 5\%$  was achieved, which would be fully sufficient for our purposes. However, we deal with two-mode system and we need to extract the signal mode which corresponds to detected idler. In the recent experimental realization of the two-mode homodyne tomography [18], the estimated efficiency was only 35%, which is below our threshold. Nevertheless, even such data may be used to demonstrate the

suppression of noise via conditional generation, although the photon number fluctuations could not be reduced below the Poissonian level.

## V. CONCLUSIONS

We have proposed a simple scheme for conditional generation of sub-Poissonian light from the two-mode squeezed vacuum. The scheme involves homodyne detection on the idler mode and the experimental run is accepted only if the absolute value of the detected quadrature is higher than certain threshold. As the threshold is increased, the photon-number fluctuations of conditionally generated state of signal mode are gradually suppressed but the probability of generation decreases. If we wish to prepare a nonclassical state with a given negative Mandel  $Q$ -factor, then we can choose an optimal squeezing parameter  $\lambda$  leading to maximum generation probability. Nonclassical light can be prepared only when the efficiency of homodyne detection  $\eta$  is higher than  $\eta_{\text{th}} \geq 1/2$ . Although the threshold  $1/2$  was not achieved in the recent experiment on two-mode homodyne tomography [18], the condition  $\eta > \eta_{\text{th}}$  is by no means severe and the present method may become experimentally feasible in a near future.

## ACKNOWLEDGMENTS

I would like to thank J. Peřina, R. Filip and L. Miřta, Jr. for valuable comments. This work was supported by Grant LN00A015 of the Czech Ministry of Education.

- [8] G. Harel, G. Kurizki, J. K. McIver, and E. Coutsias, Phys. Rev. A **53**, 4534 (1996).
- [9] A.I. Lvovsky, H. Hansen, T. Aichele, O. Benson, J. Mlynek, and S. Schiller, arXiv: quant-ph/0101051.
- [10] M.G.A. Paris, arXiv: quant-ph/0102044.
- [11] P.R. Tapster, J. G. Rarity, and J.S. Satchell, Phys. Rev. A **37**, 2963 (1988).
- [12] J.G. Walker and E. Jakeman, Opt. Acta **32**, 1303 (1985); J.G. Rarity, P.R. Tapster, and E. Jakeman, Opt. Comm. **62**, 201 (1987).
- [13] B. Schumaker and C.M. Caves, Phys. Rev. A **31**, 3093 (1985).
- [14] O. Aytür and P. Kumar, Phys. Rev. Lett. **65**, 1551 (1990).
- [15] L. Mandel and E. Wolf, *Optical Coherence and Quantum Optics*, (Cambridge University Press, Cambridge, 1995).
- [16] U. Leonhardt and H. Paul, Prog. Quant. Electr. **19**, 89 (1995).
- [17] S. Schiller, G. Breitenbach, S.F. Pereira, T. Müller, and J. Mlynek, Phys. Rev. Lett. **77**, 2933 (1996).
- [18] M. Vasilyev, S.-K. Choi, P. Kumar, and G.M. D'Ariano, Phys. Rev. Lett. **84**, 2354 (2000).

- 
- [1] M. Ban, Phys. Rev. A **49**, 5078 (1994); J. Mod. Opt. **43**, 1281 (1996).
  - [2] K. Watanabe and Y. Yamamoto, Phys. Rev. A **38**, 3556 (1988); M. Ban, Phys. Lett. A **233**, 284 (1997).
  - [3] A. Luis and L.L. Sánchez-Soto, Phys. Lett. A **244**, 211 (1998).
  - [4] K. Vogel, V. M. Akulin, and W. P. Schleich, Phys. Rev. Lett. **71**, 1816 (1993).
  - [5] J. I. Cirac, R. Blatt, A.S. Parkins, and P. Zoller, Phys. Rev. Lett. **70**, 762 (1993); O. Steuernagel, Opt. Commun. **138**, 71 (1997); G. M. D'Ariano, L. Maccone, M.G.A. Paris, and M.F. Sacchi, Phys. Rev. A **61**, 053817 (2000).
  - [6] S. Song, C.M. Caves, and B. Yurke, Phys. Rev. A **41**, 5261 (1990); B. Yurke, W. Schleich, and D.F. Walls, Phys. Rev. A **42**, 1703 (1990).
  - [7] M. Dakna, T. Anhut, T. Opatrny, L. Knöll and D.-G. Welsch, Phys. Rev. A **55**, 3184 (1997); J. Clausen, M. Dakna, L. Knöll, and D.-G. Welsch, J. Opt. B: Quant. Semiclass. Opt. **1**, 332 (1999).